

## Corrosion Resistance of Ni/Al<sub>2</sub>O<sub>3</sub> Nanocomposite Coatings

Beata KUCHARSKA, Agnieszka BROJANOWSKA, Karol POPLAWSKI,  
Jerzy Robert SOBIECKI\*

The Faculty of Materials Science and Engineering, Warsaw University of Technology, 02-507 Warsaw, Woloska 141, Poland

**crossref** <http://dx.doi.org/10.5755/j01.ms.22.1.7407>

Received 23 June 2014; accepted 07 February 2015

Nickel matrix composite coatings with ceramic disperse phase have been widely investigated due to their enhanced properties, such as higher hardness and wear resistance in comparison to the pure nickel. The main aim of this research was to characterize the structure and corrosion properties of electrochemically produced Ni/Al<sub>2</sub>O<sub>3</sub> nanocomposite coatings. The coatings were produced in a Watts bath modified by nickel grain growth inhibitor, cationic surfactant and the addition of alumina particles (low concentration 5 g/L). The process has been carried out with mechanical and ultrasonic agitation.

The Ni/Al<sub>2</sub>O<sub>3</sub> nanocomposite coatings were characterized by SEM, XRD and TEM techniques. In order to evaluate corrosion resistance of produced coatings, the corrosion studies have been carried out by the potentiodynamic method in a 0.5 M NaCl solution. The corrosion current, corrosion potential and corrosion rate were determined. Investigations of the morphology, topography and corrosion damages of the produced surface layers were performed by scanning microscope techniques.

**Keywords:** nickel coating, Al<sub>2</sub>O<sub>3</sub> particles, electrodeposition, corrosion resistance, nanocomposite.

### 1. INTRODUCTION

In the last few years the interest in nanocomposite engineering metal coatings has increased rapidly. There is a few methods of producing metallic nanocomposite materials and electrodeposition is a simple, inexpensive and versatile one. Different types of inert particles with a variety of properties, such as metals, ceramics or polymers, can be used. The structure and properties of composite surface coatings can be designed through a careful selection of the matrix and dispersed phase. Among wide variety of materials used for tribological applications, nickel composite coatings containing nanometric, hard alumina particles appear to have very promising potential. Composite electroplating combined with the variety of metals that can be electrodeposited enables the production of a wide range of composite materials with improved properties in terms of wear resistance, lubrication or corrosion resistance. One of the most used composite coatings due to its high wear resistance is the Ni/Al<sub>2</sub>O<sub>3</sub> coating. Until now, most of the works were carried out using Al<sub>2</sub>O<sub>3</sub> microparticles. However, the recent emergence of nanotechnologies has lead to scientific and technological interest on the electrodeposition of Ni/Al<sub>2</sub>O<sub>3</sub> nanocomposite coatings with Al<sub>2</sub>O<sub>3</sub> particles smaller than 100 nm, mainly devoted to increase the abrasion resistance of metal surfaces [1–16].

Despite rapid advances in nanocomposite coatings research, certain aspects concerning the agglomeration of particles in the electrolyte, the low content of nanoparticles in the composite coating and the non uniformity of particles distribution in the metal matrix remain to be

solved. To cope with these problems, some attempts have been made, such as use additives as a chemical dispersion agent for the particles or to use pulse plating in order to enhance co-deposition of particles and improve homogeneity. Another possibility is to apply ultrasonic energy. By appropriate selection of the powder type, its volumetric share in the electrolyte and its process parameters, such as: the composition of the electrolyte, current density or hydrodynamic conditions during the electrodeposition process, a layer with valuable performance characteristics can be produced [3–5, 8, 10, 11, 14].

Apart of increased wear resistance, heat resistance and hardness, deposited Ni/Al<sub>2</sub>O<sub>3</sub> coatings should also have good anticorrosion properties, especially if they are destined to work in aggressive media. The second-phase particles, present in the electroplating bath and then in the coating are responsible for the surface properties, which affect its corrosion behaviour [6].

The fact that the second-phase particles affect the nickel composite coating's surface morphology and protective properties in different ways and degrees is the reason why the corrosion test results for coatings Ni/Al<sub>2</sub>O<sub>3</sub> are often inconsistent. The researchers concentrate on corrosion rate determination. There is a lack of reports on the causes of the changes in the protective properties and how they are related to structural changes and no attempts have been made to describe the mechanism of the corrosion destruction of composite coatings. The results and conclusions published so far in this field are few, far between and inconsistent with each other. As a result, the production of composite layers by way of electrochemical reduction requires a good diagnosis of the mechanisms and effects of these processes in order to better control many

\* Corresponding author. Tel.: +48-22-234 8451; fax: +48-22-848 48 75.  
E-mail address: [jrs@inmat.pw.edu.pl](mailto:jrs@inmat.pw.edu.pl) (J.R. Sobiecki)

factors shaping the structure and properties of the material at the same time. One of the first stages in the undertaken study was to characterise the nanometric alumina powder used and determine the optimal hydrodynamic parameters in a bath with low Al<sub>2</sub>O<sub>3</sub> concentration in order to obtain a layer with evenly distributed alumina [1, 9].

## 2. EXPERIMENTAL DETAILS

Nickel matrix composite coatings with a low content dispersed Al<sub>2</sub>O<sub>3</sub> phase (Aldrich Chemistry) were produced by electrochemical reduction on a copper substrate (75 × 15 × 1) in a Watts bath modified with benzoic sulfimide (saccharin) and a cationic surfactant (Table 1). The nickel and composite coatings have a thickness of approximately 30 μm, with the exception of the coatings to be examined by TEM technique (150–200 μm), which preparation've differed from the conventional procedure (additional application of electrospark cutting, grinding to a thickness of 4 μm and electrochemical polishing). Electrodeposition process consists of several steps and is shown schematically in Fig. 1.

**Table 1.** Bath composition and plating conditions for Ni/Al<sub>2</sub>O<sub>3</sub> composite coatings

Component	Concentration, g·L <sup>-1</sup>
NiSO <sub>4</sub> · 6 H <sub>2</sub> O	300
NiCl <sub>2</sub> · 6 H <sub>2</sub> O	40
H <sub>3</sub> BO <sub>3</sub>	35
Saccharin	5
Al <sub>2</sub> O <sub>3</sub>	5
Plating conditions	Value
pH	4.2
Temperature, °C	45
Current density, A/dm <sup>2</sup>	3

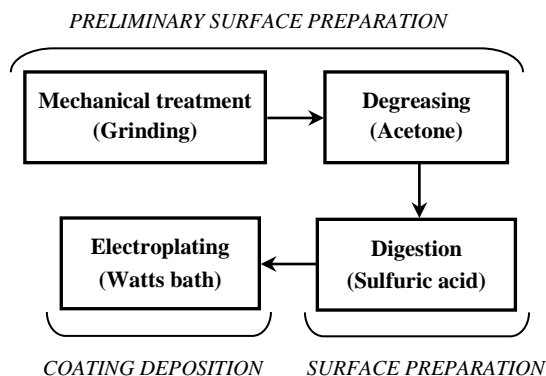


**Fig. 1.** Scheme for preparing nickel and composite coatings

In order to facilitate the transport of ceramic phase particles into cathode proximate areas, the bath was subjected to mechanical stirring (MS) at 500 rpm or ultrasound stirring (US). Analysis of the Al<sub>2</sub>O<sub>3</sub> structure, the nickel coatings and the Ni/Al<sub>2</sub>O<sub>3</sub> composite coatings was carried out using a Hitachi SU-70 scanning electron microscope (SEM) and a JEOL JEM 1200 EX II transmission electron microscope (TEM).

In order to determine the phase composition of the deposited coatings, X-ray diffraction (XRD) measurements were performed using a Rigaku MiniFlex II diffractometer ( $\lambda = 0.154$  nm).

Examinations of corrosive properties of nickel and composite Ni/Al<sub>2</sub>O<sub>3</sub> coatings were made with the use of potentiostat ATLAS Sollich 0531EU&IA, and AtlasCorr v. 5.0 computer program while the examination results were performed with a AtlasLab v. 2.0 program. Three-electrode measurement system comprised a measurement vessel where saturated calomel electrode (NEK) playing a role of reference electrode and platinum mesh as a counter electrode were placed. Copper with Ni and Ni/Al<sub>2</sub>O<sub>3</sub> coatings constituted the third working electrode.

Corrosion resistance was tested in the 0.5M NaCl solution at 20 °C.

The samples, before testing corrosive properties of produced coatings, were stabilized for 60 minutes in the target system connected to the measurement set as an open system.

To perform the corrosion tests the potentiodynamic method was used. For determining polarization curves of the tested materials the measurements started from the potentials having values lower by 200 mV up to the values higher by 200 mV from the predetermined open system potential with the potential change velocity equal to 0.2 mV/s and then up to 500 mV with velocity of 0.8 mV/s. The obtained curves were analyzed by Tafel straight lines method with keeping the conditions inherent in this method.

## 3. RESULTS AND DISCUSSION

Alumina powder containing nanometric amorphous and nanocrystalline fractions of particles with heterogeneous grain size from 5 nm to 100 nm (Fig. 2) was used as the dispersed phase in the Ni/Al<sub>2</sub>O<sub>3</sub> composite coating formation process.

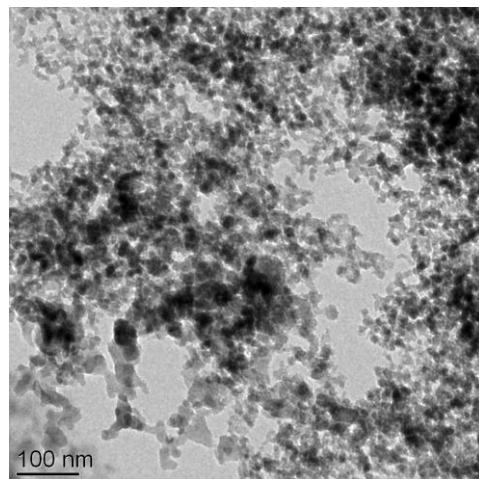


**Fig. 2.** TEM image of Al<sub>2</sub>O<sub>3</sub> powder

The quality of the composite material with a nickel matrix and alumina dispersed phase depends on both the selection of components, as well as formation of an appropriate structure, which would ensure the right interaction between the materials making up the composite.

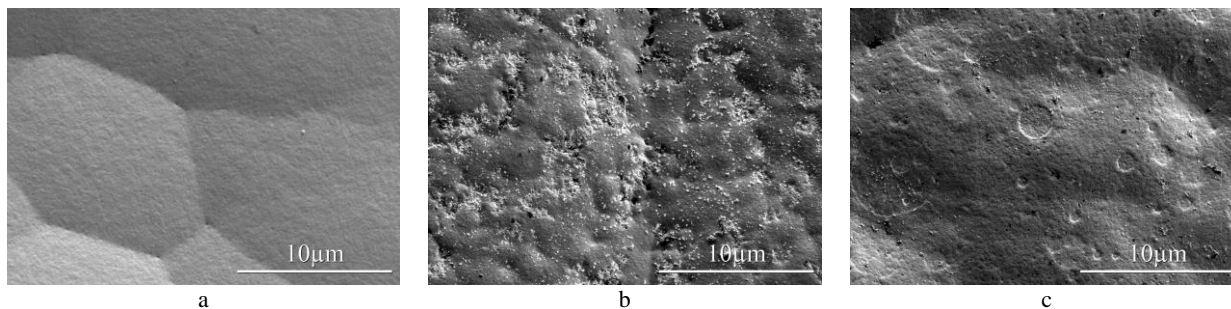
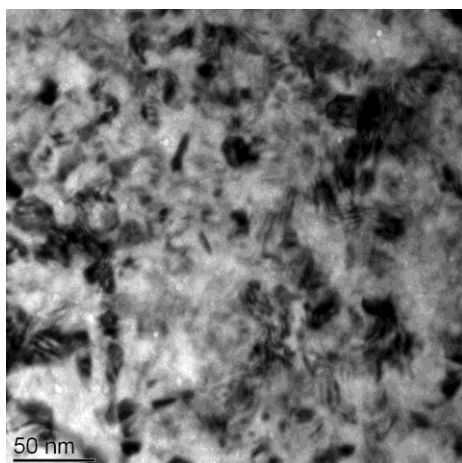
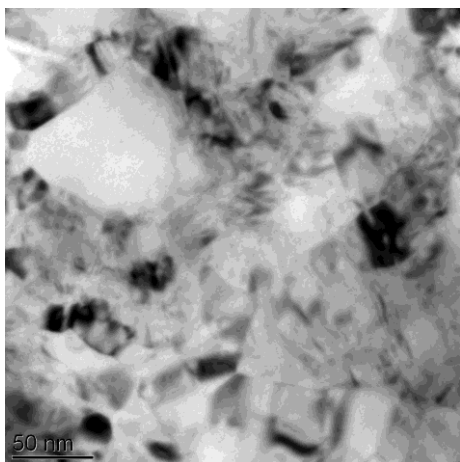


**Fig. 3.** Morphology of nanocrystalline coatings: a – nickel coating; b – Ni/Al<sub>2</sub>O<sub>3</sub> coatings produced using mechanical stirring; c – Ni/Al<sub>2</sub>O<sub>3</sub> coatings produced using ultrasonic stirring

The Al<sub>2</sub>O<sub>3</sub> particles being embedded in the nickel layer cause a significant change in the morphology of its surface (Fig. 3 a–c).



a



b

**Fig. 4.** TEM image of the structure: a – of the nickel coating material; b – of the Ni/Al<sub>2</sub>O<sub>3</sub> composite coating material

The largest number of Al<sub>2</sub>O<sub>3</sub> particles, which are only partly embedded but well fixed and distributed in the nickel matrix, can be observed on the surface of the composite layer produced using mechanical stirring at 500 rpm (Fig. 3 b). Ni/Al<sub>2</sub>O<sub>3</sub> coatings produced using ultrasonic stirring (Fig. 3 c) demonstrate good ceramic agglomeration break-up but also large surface roughness, which is caused by pressure variations (effect of cavitation) during the application of ultrasound. All the investigated coatings were characterized by a cohesive texture, uniform thickness (except the edges) and did not show any discontinuity.

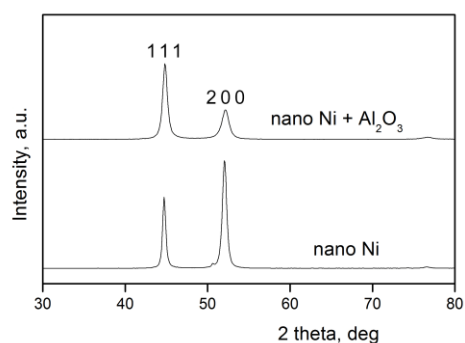


**Fig. 5.** XRD patterns for deposited Ni layer and the same Ni layers containing nanoparticles of Al<sub>2</sub>O<sub>3</sub>

The microstructure of the nickel and Ni/Al<sub>2</sub>O<sub>3</sub> coatings obtained in the bath with mechanical stirring were examined by TEM technique (Fig. 4).

Nickel grains have very clear boundaries (Fig. 4 a), in contrast to nanocrystalline composite coatings (Fig. 4 b), where the boundaries between the particular grains are blurred. In the case of nanocrystalline nickel coatings, grain boundaries are not very clearly visible. In all the examined materials, the existence of defects (twinned grains) in the structure is observed.

XRD patterns for the deposited Ni coating and the composite Ni/Al<sub>2</sub>O<sub>3</sub> coating produced with mechanical stirring are shown in Fig. 5. Significant broadening of the diffraction lines of Ni are visible, testifying to its nanocrystalline structure. The crystallite size (broadening of the XRD line) decreases in the case of composite coating because of presence of surfactant, which is expedient in Watts bath, in which the particles are suspended. The diffraction lines of Al<sub>2</sub>O<sub>3</sub> are not recorded due to the small content of these phases in the composite layer. Moreover, evidence of texture in the case of the nanocrystalline Ni layer is seen, since the intensity of the (200) diffraction line is higher than the (111) line.

Fig. 6 shows the course of corrosive potential of nickel and composite coatings changes during 60 min., in the open arrangement, whereas in Table 2 characteristic values read off from these curves are presented. The tests revealed that Ni/Al<sub>2</sub>O<sub>3</sub> composite coatings deposited with mechanical stirring decrease their corrosion potential in the open arrangement in comparison of pure nickel. The potential of composite coating Ni/Al<sub>2</sub>O<sub>3</sub> obtained with ultrasonic agitation is increased to the value -154 mV (Table 2). Potentiodynamic tests revealed that nickel and composite coatings deposited with ultrasound stirring have similar corrosion properties, while the Ni/Al<sub>2</sub>O<sub>3</sub> coatings

are characterized by decreased corrosion potential (-222 mV) and current density ( $0.77 \mu\text{Acm}^{-2}$ ).

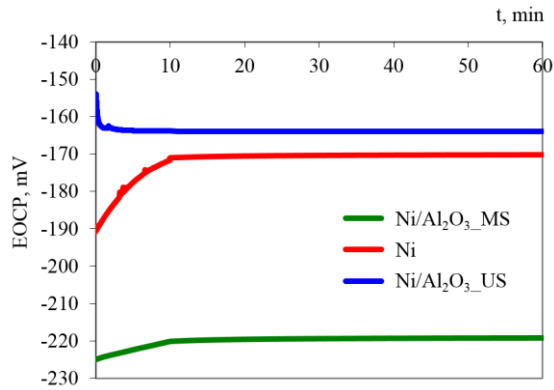


**Fig. 6.** Potential changes over time (60 min) of Ni and Ni/Al<sub>2</sub>O<sub>3</sub> coatings deposited with different hydrodynamic parameters

**Table 2.** Characteristic values obtained as a result of open circuit potential measurement

Material	$E_0$ , mV	$E_f$ , mV	$E_{max}$ , mV	$E_{min}$ , mV
Ni	-191	-170	-170	-191
Ni/Al <sub>2</sub> O <sub>3</sub> _MS	-225	-219	-225	-219
Ni/Al <sub>2</sub> O <sub>3</sub> _US	-154	-164	-154	-164

It was also demonstrated that in the case of composite coatings, the values of current density was decreased relative to nickel coating. This is due to non-conductive nature of alumina: the higher the value of co-deposited ceramic phase, the lower the value of corrosion current density.

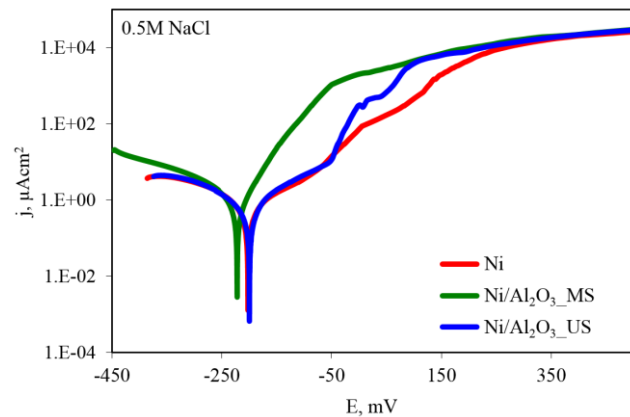


**Fig. 7.** Polarization curves of Ni and Ni/Al<sub>2</sub>O<sub>3</sub> coatings deposited with different hydrodynamic parameters

Polarization resistance values  $R_{pol}$  (Fig. 8) show that the deterioration of corrosion resistance is the highest in the case composite coating deposited with mechanical stirring ( $33.99 \text{ k}\Omega\text{cm}^2$ ). Fig. 7 presents the results of potentiodynamic method examinations. The characteristic values are presented in Table 3. Corrosive potential and corrosion current density were evaluated by Tafel's

method, while polarization resistance was determined by Stern equation and presented in Fig. 8. Analyses of electrodeposited nickel and composite coatings after exhibited in corrosion environments have demonstrated a pitting corrosion on surfaces of electrodeposited materials (Fig. 9 a–c). Together with increase of co-deposited alumina the greater etching is visible (Fig. 9 b, c).

**Table 3.** Characteristic parameters obtained as a result of potentiodynamic tests

Material	$E_{corr}$ , mV	$i_{corr}$ , $\mu\text{Acm}^{-2}$	$R_{pol}$ , $\text{k}\Omega\text{cm}^2$
Ni	-203	2.2	27.96
Ni/Al <sub>2</sub> O <sub>3</sub> _MS	-222	0.77	10.31
Ni/Al <sub>2</sub> O <sub>3</sub> _US	-199	1.2	33.99

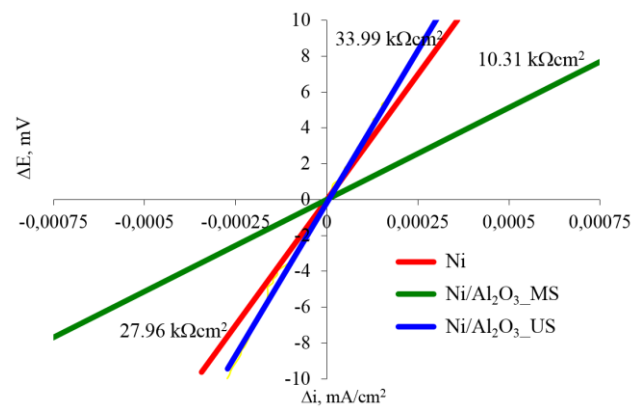


**Fig. 8.** Applied current linear polarization curve

## 4. CONCLUSIONS

1. Ni and composite Ni/Al<sub>2</sub>O<sub>3</sub> coatings produced in a Watts bath by means of electrocrystallisation are characterised by a nanocrystalline structure of nickel.
2. Mechanical agitation at 500 rpm ensures the best dispersion of Al<sub>2</sub>O<sub>3</sub> on the surface and produces the hardest coating.
3. Ultrasound agitation leads to significant surface development, a high degree of agglomerate break-up but insufficient amounts of embedded Al<sub>2</sub>O<sub>3</sub>, which translates into the best corrosion properties.
4. The coating Ni/Al<sub>2</sub>O<sub>3</sub> deposited with ultrasonic agitation has the best corrosion properties (the highest corrosion potential and polarization current density).
5. The incorporation of non-conductive Al<sub>2</sub>O<sub>3</sub> particles in the nickel matrix decreases the corrosion current.

## Acknowledgments

The study was performed in the framework of the research project of the National Science Center entitled "Composite nanomaterials produced by electrochemical method" (2012/05/B/ST8/01555).

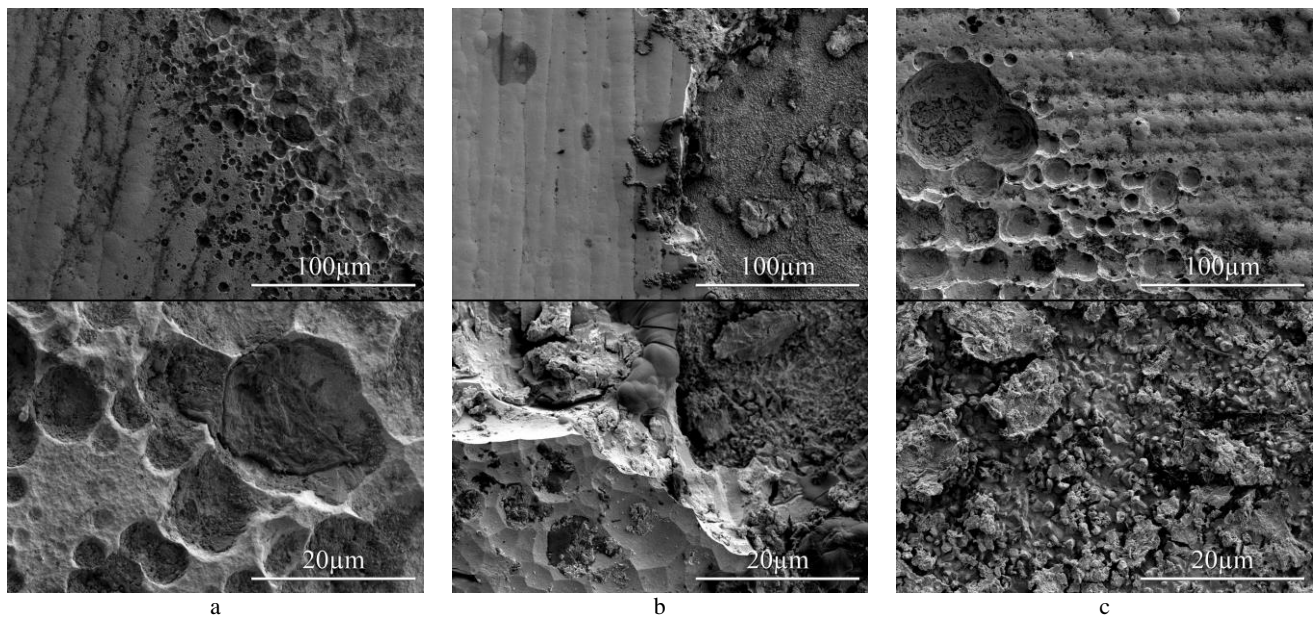


**Fig. 9** SEM images of the structure destruction after corrosion tests of examined materials: a – nickel coatings; b – Ni/Al<sub>2</sub>O<sub>3</sub> coatings produced using mechanical stirring; c – Ni/Al<sub>2</sub>O<sub>3</sub> coatings produced using ultrasonic stirring

## REFERENCES

1. **Szczygiel, B., Kolodziej, M.** Composite Ni/Al<sub>2</sub>O<sub>3</sub> Coatings and Their Corrosion Resistance *Electrochimica Acta* 50 2005: pp. 4188–4195.
2. **Schlesinger, M., Paunovic, M.** Modern Electroplating. Wiley, 2010: pp. 79–114.  
<http://dx.doi.org/10.1002/9780470602638>
3. **Hovestad, A., Janssen, L.J.J.** Electrochemical Codeposition of Inert Particles in a Metallic Matrix *Journal of Applied Electrochemistry* 25 1995: pp. 519–527.
4. **Wang, Sh., Wei, W. J.** Kinetics of Electroplating Process of Nano-sized Ceramic Particle/Ni Composite *Materials Chemistry and Physics* 78 2003: pp. 574–580.  
[http://dx.doi.org/10.1016/S0254-0584\(01\)00564-8](http://dx.doi.org/10.1016/S0254-0584(01)00564-8)
5. **Spyrelli, N., Pavlatou, E., Spanou, A., Zoikis-Karathanasis, A.** Nickel and Nickel-Phosphorous Matrix Composite Electrocoatings *Transactions of Nonferrous Metals Society of China* 19 2009: pp. 800-804.  
[http://dx.doi.org/10.1016/S1003-6326\(08\)60353-2](http://dx.doi.org/10.1016/S1003-6326(08)60353-2)
6. **Feng, Q., Li, T., Yue, H., Qi, K., Bai, F., Jin, J.** Preparation and Characterization of Nickel Nano-Al<sub>2</sub>O<sub>3</sub> composite Coatings by Sediment Co-deposition *Applied Surface Science* 254 2008: pp. 2262–2268.
7. **Aruna, S., Diwakar, S., Jain, A., Rajam, K.** Comparative Study on the Effect of Current Density on Ni and Ni–Al<sub>2</sub>O<sub>3</sub> Nanocomposite Coatings Produced by Electrolytic Deposition *Surface Engineering* 21 (3) 2005: pp. 209–214.
8. **García-Lecina, E., García-Urrutia, I., Díez, J. A., Morgiel, J., Indyka, P.** A Comparative Study of the Effect of Mechanical and Ultrasound Agitation on the Properties of Electrodeposited Ni/Al<sub>2</sub>O<sub>3</sub> Nanocomposite Coatings *Surface and Coatings Technology* 206 2012: pp. 2998–3005.  
<http://dx.doi.org/10.1016/j.surfcoat.2011.12.037>
9. **Thiemig, D., Bund, A., Talbot, J.B.** Influence of Hydrodynamics and Pulse Plating Parameters on the Electrodeposition of Nickel-alumina Nanocomposite Films *Electrochimica Acta* 54 2009: pp. 2491–2498.
10. **Chengyu, T., Hang, C., Wei, H., Yu, L., Ziqiao, Z.** Influence of Nano-Al<sub>2</sub>O<sub>3</sub> Particles on Nickel Electrocrystallization at Initial Stage *Rare Metal Materials and Engineering* 39 (1) 2010: pp. 10–16.
11. **Chen, J.** Characteristic of Ni–Al<sub>2</sub>O<sub>3</sub> Nanocomposition Coatings *Procedia Engineering* 15 2011: pp. 4414–4418.  
<http://dx.doi.org/10.1016/j.proeng.2011.08.829>
12. **Wu, Z., Shen, B., Liu, L.** Effect of α-Al<sub>2</sub>O<sub>3</sub> Coatings on the Interface of Ni/SiC Composites Prepared by Electrodeposition *Surface and Coatings Technology* 206 (14) 2012: pp. 3173–3178.
13. **Beltowska-Lehman, E., Goral, A., Indyka, P.** Electrodeposition and Characterization of Ni/Al<sub>2</sub>O<sub>3</sub> Nanocomposite Coatings *Archives of Metallurgy and Materials* 56 (4) 2011: pp. 919–931.  
<http://dx.doi.org/10.2478/v10172-011-0101-1>
14. **Kucharska, B., Sobiecki, J. R.** Microcrystalline and Nanocrystalline Nickel Layers Reinforced by Al<sub>2</sub>O<sub>3</sub> Particle *Composites Theory and Practice* 13 (4) 2013: pp. 232–236.
15. **Gul, H., Kilic, F., Aslan, S., Alp, A., Akbulut, H.** Characteristics of Electro-co-deposited Ni–Al<sub>2</sub>O<sub>3</sub> Nanoparticle Reinforced Metal Matrix Composite (MMC) Coatings *Wear* 267 2009: pp. 976–990.  
<http://dx.doi.org/10.1016/j.wear.2008.12.022>
16. **Saha, R. K., Khan, T. I.** Effect of Applied Current on the Electrodeposited Ni–Al<sub>2</sub>O<sub>3</sub> Composite Coatings *Surface and Coatings Technology* 205 2010: pp. 890–895.  
<http://dx.doi.org/10.1016/j.surfcoat.2010.08.035>